Boron Nitride Nanotubes and Nanosheets

Dmitri Golberg,* Yoshio Bando, Yang Huang, Takeshi Terao, Masanori Mitome, Chengchun Tang, and Chunyi Zhi

International Center for Materials Nanoarchitectonics (MANA), National Institute for Materials Science (NIMS), Namiki 1-1, Tsukuba, Ibaraki 3050044, Japan

REVIEW

ABSTRACT Hexagonal boron nitride (h-BN) is a layered material with a graphite-like structure in which planar networks of BN hexagons are regularly stacked. As the structural analogue of a carbon nanotube (CNT), a BN nanotube (BNNT) was first predicted in 1994; since then, it has become one of the most intriguing non-carbon nanotubes. Compared with metallic or semiconducting CNTs, a BNNT is an electrical insulator with a band gap of *ca.* 5 eV, basically independent of tube geometry. In addition, BNNTs possess a high chemical stability, excellent mechanical properties, and high thermal conductivity. The same advantages are likely applicable to a graphene analogue—a monatomic layer of a hexagonal BN. Such unique properties make BN nanotubes and nanosheets a promising nanomaterial in a variety of potential fields such as optoelectronic nanodevices, functional composites, hydrogen accumulators, electrically insulating substrates perfectly matching the CNT, and graphene lattices. This review gives an introduction to the rich BN nanotube/nanosheet field, including the latest achievements in the synthesis, structural analyses, and property evaluations, and presents the purpose and significance of this direction in the light of the general nanotube/nanosheet developments.

KEYWORDS: boron nitride · nanotubes · nanosheets · chemical vapor deposition · transmission electron microscopy · atomic force microcopy

One- and two-dimensional nanostructures defined as those having at least one dimension between 1 and 100 nm have attracted a prime attention over the past two decades due to their peculiar and fascinating properties and a wide range of interesting potential applications which, in many cases, shall be more fruitful than for the corresponding bulky material counterparts. The ability to generate such minuscule structures is essential for many branches of the modern science and technology. The original findings of carbon nanotubes (CNTs)[1] in the mid-1970s followed by their complete identification in 1991[2] stimulated intense theoretical and experimental studies in regard to other nanostructures based on similar honeycomb-like networks. Layered boron nitride is a structural analogue of graphite in which alternating B and N atoms substitute for C atoms.[3,4] In general, a BN nanotube[5−9] can easily be imagined as a rolled graphite-like BN sheet, where C atoms are fully substituted by N and B atoms in a fashion shown in Figure 1. It is seen that, structurally, it is a very close analogue of the CNT. Recent rise of a carbon monatomic sheet, named graphene,[10] has also brought to the research forefront a question of the existence and stability of its BN counterpart—a monatomic graphene-like sheet solely made of B and N atoms (Figure 1).

Undisputedly, compared to its sister system (C), both the BN nanotubes and nanosheets have remained much less explored. In fact, the number of BN-related publications is notably smaller relative to the well-explored C system (Figure 2). Since the BN nanosystems have distinct differences/advantages compared to those of C, for example, they are electrically insulating (a band gap of ∼5−6 eV),[11,12] have profound chemical and thermal stabilities,[13,14] but at the same time are equally thermally conductive and mechanically robust as their C counterparts, such a shortage of studies does not reflect a fact that the BN system has been ignored and/or underestimated relative to the C nanomaterials; rather, this is primarily due to the fact that the well-defined synthesis of BN-based nanostructures is a much more challenging task compared to the case of C. All well-established synthetic routes of C nanotubes and graphene formation have not properly worked for the BN nanostructures.

Boron Nitride Nanomorphologies. BNNTs may crystallize in single- and multiwalled structures. The sheets may also be mono- or several layers thick. The single-walled BNNTs have been rather rarely observed and studied[15] compared with popular single-walled CNTs. A single-walled structure is not typical in the BNNT system due to peculiar B−N stacking characteristics. Also, in spite of a

*Address correspondence to golberg.dmitri@nims.go.jp.

Published online May 12, 2010.
10.1021/nn1006495

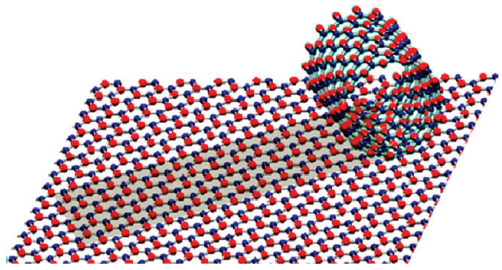

Figure 1. Structural model of a single-layered BN nanotube made through wrapping of a planar monatomic BN nanosheet. The alternating B and N atoms are shown in blue and red, respectively.

long history and rich experience in growing BN thin films,[16−26] until now, it has been rather challenging to prepare monatomic BN graphene-like layers.[27−35] Compared with the covalent C−C bonding in CNTs and graphene, the B−N bonding possesses a partially ionic character. This leads to the prominent, so-called "lip−lip" interactions between neighboring BN layers. The B and N atoms are in succession superposed along the *c* axis and prefer to form double- or multilayered tubular structures or multilayered graphite-like flakes. Formation of multilayers stabilizes the whole structure. By contrast, in graphene, the interactions between neighboring C layers are rather weak and are represented by the van der Waals forces, and this makes the formation of single-walled CNTs and monolayer graphenes much easier. In a typical BN MWNT or a multilayer flake, the tube walls/sheet layers are ordered with an interlayer distance of *ca.* 0.33−0.34 nm, characteristic of the d_{0002} spacing in a hexagonal BN. Some of the researchers reported that the interlayer spacing of BN nanotubes may be slightly larger than that of bulk h-BN (that is, ∼0.333 nm), which might result from the inner stresses within the bent walls. Similar phenomena have also been observed in CNTs.

VOCABULARY: **Boron nitride** – an inorganic compound with a chemical formula BN, consisting of equal numbers of boron and nitrogen atoms. BN is isoelectronic to a similarly structured carbon lattice and thus exists in various crystalline forms. The hexagonal form corresponding to graphite is the most stable and softest among BN polymorphs · **Nanotube** – a nanometer-scale tube-like structure. It usually refers to a *carbon* nanotube, but may also exist in many inorganic compounds, such as metal oxides, nitrides, sulfides, selenides, *etc.* · **Graphene** – a one-atom-thick planar sheet of sp^2-bonded carbon atoms that are densely packed in a honeycomb crystal lattice

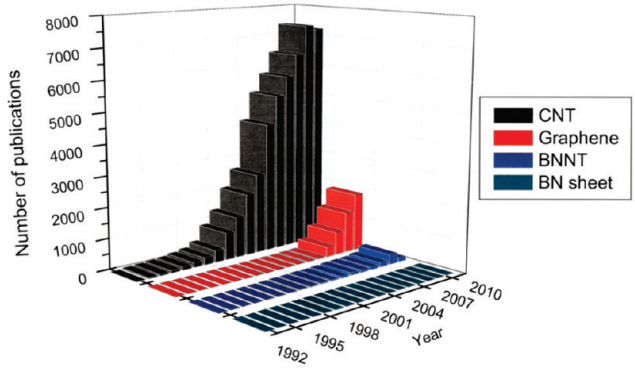

Figure 2. Diagrams showing comparative statistics of papers published year by year and related to CNT (black bars), graphene (red bars), BNNT (blue bars), and BN nanosheets (dark green bars). Data analysis based on the Scopus database, as of 02/2010.

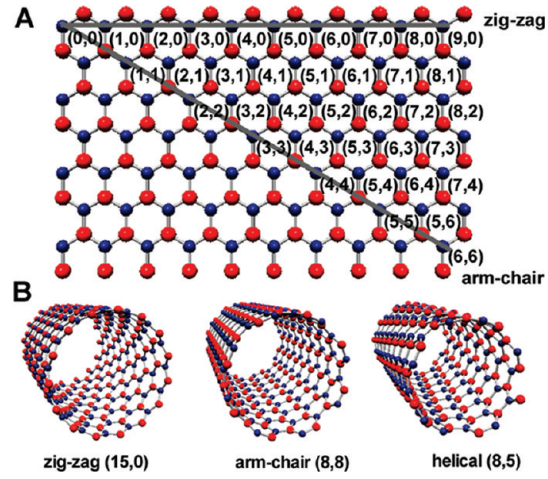

Figure 3. (A) Plane BN sheet with possible wrapping fashions and the corresponding (*n*,*m*) indices. (B) Ball and stick structural models of three types of single-walled BNNTs made of a wrapped BN layer: zig-zag (15,0), arm-chair (8,8), and a helical (8,5) tube. The B and N atoms are shown in red and blue, respectively.

Chiralities and Stackings in BNNTs. Boundary conditions after one rotation around a flat sheet axis give a limited number of choices for the helicity of a hexagonal layer relative to the tube axis. There are several cases of the tube helicities: "zig-zag" type, in which the [10−10] direction of the graphitic sheet is parallel to the tube axis; "arm-chair" type, in which the [11−20] orientation of the sheet is parallel to the axis; and many helical types with varying chiral angles (Figure 3). Such constructions are equally possible for both CNTs and BNNTs. Although arm-chair and helical tubes were also observed in BNNTs, the majority of tubes studied by many researchers displayed zig-zag or near zig-zag configurations. This is quite distinct from the standard CNTs in which all helicities are statistically equally probable.

In the case of multiwalled BNNTs or several layers thick BN sheets, a marked character is that all of the layers within an individual nanotube/nanosheet tend to have the same layouts. Crystallization of BN layers is governed by the strong tendency to have the atomically perfect B−N stacked consecutive layers, resembling the three-dimensional bulky BN crystal ordering (Figure 4). In contrast, in multiwalled CNTs, a relative freedom in a rotational disorder between neighboring C shells can lead to a wide variety of helicities. Such feature of grouped selective helical angles within a multiwalled BNNT and the symmetry of multilayer sheets can lead to the two unique stacking orders, either hexagonal- or rhombohedral-like stackings. This is quite different from the cases of multiwalled CNTs and multi-

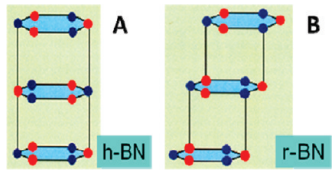

Figure 4. Three-dimensional structural models of two possible BN layer stackings in BN nanotubes/nanosheets: (A) hexagonal-like stacking; and (B) rhombohedral-like stacking.

layer graphene-based structures which allow much disordering between the consecutive shells/layers.

Cross Sections and Tip-Ends of Tubes. Polygonization of cross sections is favorable in the multiwalled BNNTs since the B−N−B−N stacking order across a BN tube could be easily preserved within the multiple polygonized shells with flat-like facets.[36] In cylindrical tubes, such stacking would be eventually broken due to various circumferences in consecutive layers. In fact, many taken TEM images of multiwalled BNNT cross sections have displayed more or less faceted-like shapes.[36] The diverse cross sections of BNNTs are related to the different growth conditions, which also determine the wall thicknesses and tube diameters. Usually in multiwalled tubes, the dark (or bright) spots can be observed on both wall sides in bright- (or dark-) field imaging modes.[37,38] Such contrasts in wall domains reflect the tube areas where strain−stress fields exist due to possibly various cross-sectional and/or chirality shell packages within the multiwalled structure. The corresponding electron diffraction patterns also exhibit additional spots which are not allowed in a perfectly cylindrical nanotube but should appear in a faceted, polygon-like cross-sectional multilayer nanostructure. Recently, a polygonal model for layered inorganic nanotubes, including those of BN, has been reviewed.[39]

Another important structural feature is that there is a striking difference in the topological defects between C and BN systems. They are namely odd-membered atomic rings in the C system, but even-membered atomic rings in the BN. These defects lead to a graphitic-like layer curling and/or full closure.

Therefore, the tips of BNNTs possess characteristic shapes that are easily distinguishable from those of CNTs. In graphite, an energetically favorable defect is a five-membered ring defect, a pentagon. The tips of CNTs are closed by introducing pentagons into the hexagonal network, six pentagons for each tip. Heptagons can also be introduced together with additional pentagons. By contrast, in a layered BN, the presence of a five-membered ring defect requires the existence of B−B and/or N−N bonds, which are energetically less favorable than a B−N bond. Therefore, in a BN layered system, squares and/or octagons normally form (Figure 5B). The presence of four-membered rings (B_2N_2 squares) at the BNNT tips, instead of five-membered rings, often leads to the formation of a flat tip with

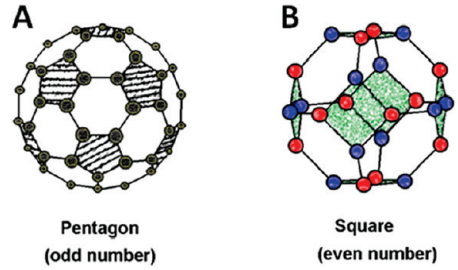

Figure 5. Typical fullerene-like molecules (A) in the carbon system (C_{60}) and (B) in the boron nitride system ($B_{12}N_{12}$), showing 12 pentagons in (A) and 6 squares in (B), which induce a complete graphitic-like sheet closure.

right-angle corners. The existence of such characteristic, rarely seen in CNTs, was initially prescribed as the distinguishing feature of BNNTs. Besides the right-angle flat tips, other tip morphologies can also be accidentally observed in BNNTs. In particular, Saito *et al.*[40] have demonstrated the tips with a triangular flag-like shape. This kind suggests that odd-numbered defects can also exist in a BN-layered system. For example, four B_2N_2 squares and two B_3N_4 (or B_4N_3) heptagons might be introduced into the hexagonal network. In addition, a triangular flag with one corner being truncated was also noticed. Such tip contains two squares, four pentagons, and two heptagons. BNNT tips might also be open.[41] The latter tip-end type was frequently observed after high-temperature chemical syntheses in oxidative atmospheres when the nonhexagonal defects had effectively been annealed out due to high atom mobility and aging/etching by oxygen-containing species or metal catalysts.

Electronic Structures. Tight-binding method was employed to compute the BNNTs' electronic structures.[11] The tubes were found to be semiconducting with direct or indirect band gaps. Theoretically, the band gap may become rather small (~2 eV) in very tiny tubes with a diameter <1 nm; however, such narrow BN tubes have never been experimentally documented. Thus, in practice, the BNNTs are supposed to be stable, electrically insulating with a rigid band gap of >5 eV. However, a flattening deformation may cause a band gap decrease.[42] The studies based on local density functional (LDA) calculations proved that it is energetically more favorable to fold a hexagonal BN sheet into a BNNT than to create a CNT from a graphite sheet.[12] According to band-folding analysis, BNNTs have a direct wide gap for zig-zag (n,0) tubes and an indirect gap for arm-chair (n,n) tubes (see Figure 3). On the other hand, strong hybridization effects may take place under folding (because a decrease in a radius of curvature); these significantly reduce the gap. For the (n,0) BNNTs with $n > 12$ (a tube diameter >0.95 nm), the hybrid states did not play a role. The gaps are stable at ~4 eV according to LDA. Because the LDA computations typically underestimate the band gap, this value coincides with the experiments. In another calculation using density func-

tional theory (DFT), the band gaps of BNNTs were found to be saturated at 5.03 eV for all tubes with realistic diameters.[43−46]

Various methods were attempted to tune the electronic structure of BNNTs, such as applying an electrical field,[47−53] strain,[54,55] doping,[56−60] introducing defects,[61−63] or modifying the tube surface.[64−66] The BNNT band gap could be directly reduced by a field or a strain or modified by introducing localized energy levels inside the gap under chemical treatments. For example, by applying an 0.2 V/Å electric field, the band gap of an arm-chair (12,12) BNNT was reduced from 4.5 to ~2.5 eV,[47] whereas fluorine doping induced an unoccupied localized state in the gap.[67] Chemical modifications enriched the properties of BNNTs; for instance, the polarization field was induced by chemical adsorption[68] or ferromagnetism by fluorine[66] or carbon doping.[69]

In double-walled BNNTs, there is hybridization between π and σ states of inner and outer tubes.[70,71] This leads to the top valence and bottom conduction band localization on the outer and inner tubes, respectively. The band gap of outer tubes is slightly narrower than for the inner tubes. This is because the downward shifts of the π states of the inner tubes are larger than that of the outer tubes. Within the interwall region, the peculiar charge redistribution is induced by the near-free-electron states.[70] Doping with fluorine significantly modified the interwall interactions and turned both layers into effective conducting channels.[72]

Between electrons and holes in BNNTs, there are strong interactions.[73,74] In fact, such excitonic effects were found to be more important in BNNTs compared to CNTs. Bright and dark excitons in BNNTs alter their optical response. For example, the absorption spectrum of a zig-zag (8,0) BNNT is dominated by a peak at 5.72 eV, due to an exciton with a binding energy of 2.3 eV.[74] The binding energy for the first excitonic peak is more than 3 eV in the arm-chair (2,2) tube, which fast converges to ~2.1 eV (peculiar to a single hexagonal BN sheet) due to the strongly localized nature of this exciton.[73]

Theoretical band gap of a BN sheet was computed to be 4.60 eV.[75] Several works have addressed the effects of vacancies on magnetic properties[76−78] and edges on electronic properties of BN layers.[52,79]

Synthesis of BN Nanotubes. The techniques known for the growth of CNTs (*e.g.*, arc-discharge and chemical vapor deposition (CVD)) have all been modified to synthesize BNNTs.[5−7] In addition, a number of alternative techniques, such as continuous laser heating at superhigh[8] or ambient pressures,[80−82] heating of milled B powders or B-containing reagent mixtures,[83] metal-boride-catalyzed CVD,[84] the so-called "substitution reaction" method,[85] high-temperature CVD,[86] low-temperature plasma-enhanced pulsed laser deposition,[87] arc-melting of LaB_6 powders,[88] heating of h-BN powders up to 2100 °C in a nitrogen atmosphere,[89] and a pressurized vapor condensed method,[90] have been developed. Nevertheless, the absence of an effective method for the large-scale synthesis of BNNTs with high purity and small diameters is still a prime obstacle in a route toward further understanding BNNT characters and their real practical prospects. In the following paragraphs, some of the most important methods developed for the synthesis of BNNTs are briefly reviewed.

The first successful synthesis of BNNTs was reported by Chopra *et al.*[5] *via* an arc-discharge procedure in 1995. BNNTs were fabricated in a plasma arc-discharge apparatus. The insulating nature of bulk BN prevented its use as an electrode. Instead, a pressed rod of h-BN was inserted into a hollow W electrode, forming a compound anode. The cathode consisted of a rapidly cooled copper electrode. The synthesized BNNTs possessed metallic nanoparticles encapsulated at the tube tip-ends, which originated from the tungsten electrode. Other developments of the arc-discharge synthesis have also been reported. For example, Loiseau *et al.*[6] used hot-pressed HfB_2 rods as electrodes to produce BNNTs. The plasma was established between HfB_2 electrodes in nitrogen atmosphere. Saito *et al.*[40] fabricated BNNTs by an arc-discharge between ZrB_2 electrodes, also in N_2 atmosphere. Altoe *et al.*[91] used conductive electrodes prepared by melting elemental B with Ni and Co and directly injected pure nitrogen gas into the plasma during arcing. However, in all of these experiments, the yield of BNNTs was rather low and the products contained various metal impurities depending on the electrode material used.

In 1996, Golberg *et al.*[8] reported on the first growth of pure BNNTs through laser heating of hexagonal and cubic BN targets at superhigh nitrogen pressure. Hexagonal or cubic BN single crystals were laser heated in a diamond anvil cell (DAC) under nitrogen pressures of 5−15 GPa. A stabilized CO_2 laser was focused onto the edge of the BN samples. The laser beam heated the targets for approximately 1 min. Temperatures above 5000 K were reached under these experimental conditions. On the surface of the laser-irradiated BN targets, pure but rather short, <100 nm, BNNTs, with outer diameters of 3−15 nm, were found.

Some years later, Laude *et al.*[81] also using a continuous CO_2 laser heating of a BN target under low nitrogen pressure produced BNNTs in a somewhat larger quantity. The synthesized tubes were self-assembled in ropes, ~40 μm long. BN-coated B nanoparticles and BN flakes were also found in the products. Similarly, Loiseau's group[15,82] reported that, through the continuous heating of a h-BN target by a continuous CO_2 laser under a partial pressure of nitrogen gas, single-walled short BNNTs, around hundreds of nanometers, could be obtained. Although there were still some multiwalled nanotubes (20%) and many B-containing nanoparticles mixed in the products, such a method seems to be the

most effective route for getting single-walled BNNTs so far. Arenal *et al.*[82] proposed a root-growth model for these single-walled BNNTs based on the TEM analyses, synthetic parameters checking, and a B−N phase diagram study. In this model, a B droplet plays an important role, and three steps were considered to be involved in the growth depending on temperature: (i) formation of liquid B droplets from the decomposition of different B compounds existing in a hexagonal BN target; (ii) reaction of these B droplets with N_2 (present in the vaporization chamber) and recombination of these elements to form BN; and (iii) incorporation of the N atoms at the root of the B particles at active reacting sites that finally leads to the tube growth.

Due to the analogous layered structures and close lattice constants between CNTs and BNNTs, the former can be used as a lattice-matching template to produce BNNTs. In fact, Han *et al.*[85] have shown that a substitution reaction starting from multiwalled CNTs is applicable for the low-cost mass production of multiwalled B−C−N and BN nanotubes on such templates. The designed reaction relies on the fact that the B and N atoms substitute for C atoms under CNT oxidation by B_2O_3 vapor in a flowing nitrogen atmosphere along with a reaction: $B_2O_3 + 3C$ (nanotubes) $+ N_2 \rightarrow 2BN$ (nanotubes) $+ 3CO$. The synthesized BNNTs had diameters and lengths similar to those of the starting CNT templates. The major drawback of this method was the residual C presence in the resultant tubes. Due to the incomplete substitution of C atoms during the reaction, a significant fraction of ternary B−C−N nanotubes existed in the products. Golberg *et al.*[95] improved this method through the additions of MoO_3 in the reactants as a promoter. The sublimated oxide vapors caused fast CNT template opening at relatively low temperatures and resulted in effective substitution of C for BN on both sides (inner and outer) of the CNT templates. A fraction of pure BNNTs was remarkably improved by using this technique. Another kind of the templates used for the growth of BNNTs was an anodic aluminum oxide (AAO) membrane. Bechelany *et al.*[96] have described a technique to synthesize BNNT arrays from a liquid polymeric borazine using AAO template channels. Thermolysis of a B precursor was carried out inside the templates using a liquid-phase infiltration (LPI) technique. The BNNTs were 60 μm long and had an average diameter of 200 nm. However, the crystallization of BNNTs was not satisfactory and the yields were still limited.

Lourie *et al.*[84] described BNNT growth by chemical vapor deposition (CVD) using a borazine ($B_3N_3H_6$) precursor. The precursor was generated *in situ* from a molten salt consisting of a mixture of $(NH_4)_2SO_4$, $NaBH_4$, and Co_3O_4 at 300−400 °C ($3(NH_4)_2SO_4 + 6NaBH_4 \rightarrow 2B_3N_3H_6 + 3Na_2SO_4 + 18H_2$). The nanotube growth was achieved from nickel boride particle catalysts. The BNNTs exhibited lengths of up to 5 μm and often possessed bulbous, flag-like and/or club-like tips. Multiwalled BNNTs were also synthesized by Ma *et al.*[86] *via* a CVD route from a $B_4N_3O_2H$ precursor. The tips encapsulated boron oxynitride nanoclusters, which incorporated Si, Al, and Ca and served as the effective promoters for the CVD growth. Later, BNNTs grown by floating catalyst CVD were reported by Kim *et al.*[92] On the basis of the use of low pressure of a molecular precursor, borazine, in conjunction with a floating nickelocene catalyst, double-walled BNNTs were fabricated. However, the product was not pure because catalytic Ni nanoparticles were frequently incorporated into the BNNT tip-ends.

Original ball milling−annealing method was pioneered by Chen *et al.*[83] Elemental B powders were first ball-milled in NH_3 atmosphere at room temperature for long times. High-energy milling impacts transferred a large amount of mechanical energy into B powder particles, leading to a metastable material composed of disordered BN and nanocrystalline B. Then the powders were subsequently heated in N_2 gas at 1200 °C to fully convert all remaining B or mixed B−N powder to BN. Large quantities of BNNTs could be obtained by this method. The shortcoming was that the prepared BNNTs usually had bamboo-like structures and the B/B−N reactants (amorphous B particles and BN bulky flakes) remained in the products. These are very difficult to remove after the synthesis because both BN and B phases are equally stable. Ball milling of a B powder followed by annealing at 1100 °C over 15 h under N_2 flow resulted in rather long BN tubular fibers.[97] The longest fiber was ~1 mm in length, while a diameter ranged from 50 to 200 nm. An attempt to produce BNNTs from B_2O_3 powder over 100 h ball milling followed by annealing at 1200 °C for 6 h under a continuous flow of ammonia again resulted in BNNTs with bamboo-like features.[98] Similar mechanothermal process was employed to grow BNNTs from h-BN powders in two steps.[99] First, the powders were ball-milled with liquid ammonia in acetone over 10−100 h under ambient conditions. This method generated highly disordered/amorphous fibers that were converted into crystalline BNNTs *via* isothermal annealing under nitrogen at 950−1300 °C for ~10 h. The longest BNNTs, ~1 μm, were produced at 1300 °C.

A few years ago, the most promising synthetic route, so-called BOCVD method, was developed within our group in Tsukuba using CVD, and a boron powder, and a metal oxide as the reactants.[93] Typically, a vertical induction furnace was used (Figure 6). The furnace had two inlets on its top and base and one outlet on its side. A mixture of B and MgO powders was loaded into a BN crucible and placed at the bottom of the reaction chamber. During the reaction process, a protecting and transporting argon flow and a reactive ammonia flow were introduced through the inlets at a flow rate of 200 (base) and 300 sccm (top) when the furnace was heated

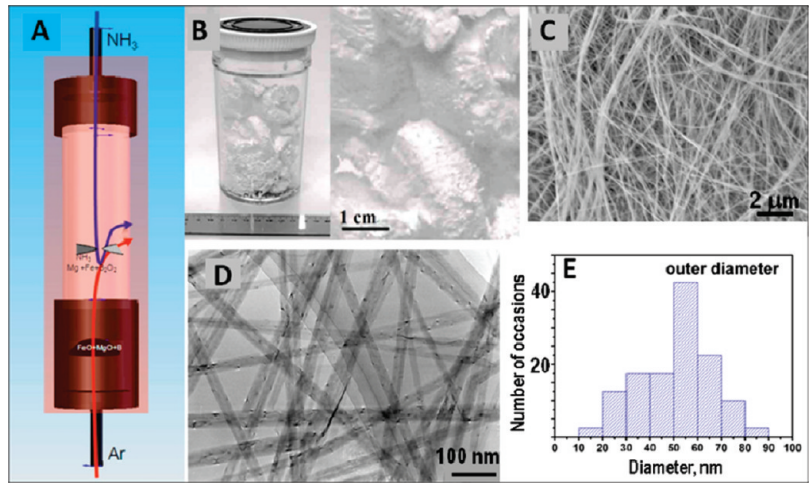

Figure 6. (A) Illustration of the apparatus for the synthesis of pure snow-white multiwalled BNNTs by the BOCVD method. (B) Photo images of as-prepared BNNT products. (C,D) Typical scanning (SEM) and transmission electron microscopy (TEM) images, displaying high yield and pure phase of a BNNT product. (E) Histograms of the tube diameter distributions.

to ~1300 °C. At this temperature, B reacted with MgO to form B_2O_2 and Mg vapor in accord with a reaction: 2B (s) + 2MgO (s) → B_2O_2 (g) + 2Mg (g). The vapors were argon-transported upwardly and reacted with a supplying NH_3 gas in the lower temperature furnace zone. After reaction for 2 h, white-colored pure BNNT products could be collected from the reaction chamber (Figure 6).

This method was further improved with respect to the larger BNNT quantities when SnO or FeO were added into the precursor mixtures.[94] The metal oxides worked as solvents at a high temperature during the reaction between B and MgO. The macro- and micromorphologies of the products are shown in Figure 6B−D. These display high yield and high purity of the tubes. Nowadays, gram levels of highly pure BNNTs can be obtained using this technique in a single experimental run. The phase purity can be up to 90 vol % and C impurities are totally eliminated. No C-containing phases are involved in the process, and additionally, the precursors and the products are well-separated during the growth. These resulted in the ultimate "snow-white" tube purity. However, it is still a challenge to control the BNNT diameters and the number of walls under this method. Most BNNTs synthesized *via* this route have a diameter of approximately 50 nm, as shown in Figure 6E.

Further developments of the regarded method along with the use of pulsed-laser deposition-coated MgO films on Si substrates, masks on them, normal BOCVD precursors and the novel growth vapor trapping (GVT) technique have enabled Yap's team to achieve a patterned growth of BNNT arrays in a simple resistive horizontal tube furnace[100] (Figure 7).

A simple chemical reaction of a mixture of nitrogen and hydrogen gas with previously ball-milled B−Ni powder at 1025 °C has recently been utilized by Lim *et al.*[102] This method successfully generated BNNTs with 20−40 nm and lengths >250 nm. The process did not involve any harmful precursors and requires comparatively low temperature.

Very recently, the researchers from NASA have developed a method named PVC (pressurized vapor/condenser) and produced highly crystalline, very long, small-diameter BNNTs without using any catalysts.[90] Palm-sized, cotton-like masses of tube raw material were grown and spun directly into centimeter-long yarns. The technique involved the forced condensation of seed particles in an ascending plume of pure B vapor (held at elevated ambient pressure; 2−20 times atmospheric pressure). The B vapor was produced at a quasi-point source by local heating (by a laser) of a target, for example, cast B, hot- or cold-pressed BN, or an amorphous BN powder, centered in the chamber. The large density difference between the hot B vapor (*T* over 4000 °C) and the surrounding high pressure N_2 gas (room temperature) generated a strong buoyancy force and a narrow vertical B vapor plume. A cooled metallic wire traversed the B plume and acted as a condenser for B droplets on which BN tubes grew under droplet collisions with molecular nitrogen supplied. Clusters of BNNT grew, intermingled, interlocked, and were shaped by fluid shear into a dimensionally stable fibril shape (Figure 8). The whole process lasted only

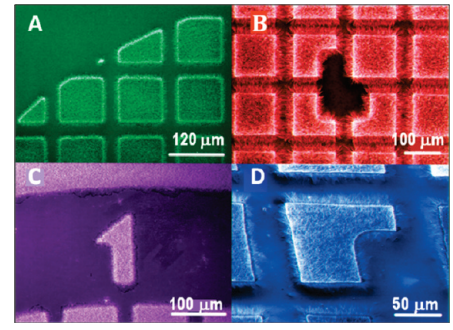

Figure 7. Well-defined patterned growth of multiwalled BNNTs on Si substrates (artificial colors are added). Adapted from ref 100.

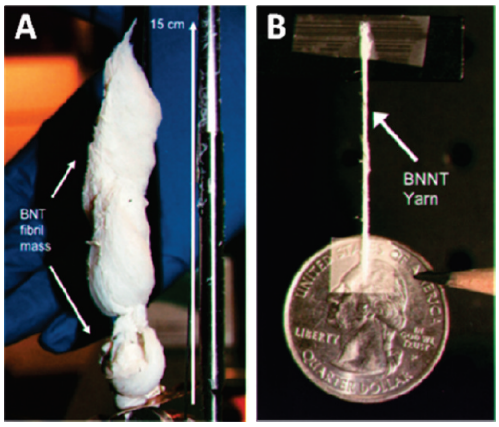

Figure 8. (A) Result of a 200 mg PVC BNNT single production run. The material has the appearance of cotton balls, though the texture is somewhat softer and the material finer-grained. (B) BNNT yarn (~1 mm diameter, 3 cm long) spun directly from the PVC-grown BNNT raw material. The BNNT fibril could readily support a small load (~a 6 g coin). Adapted from ref 90.

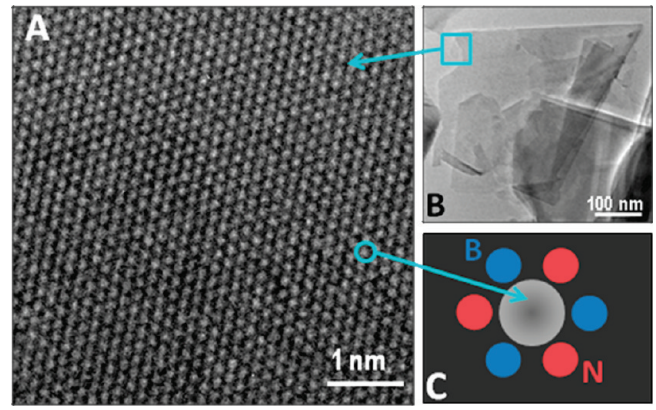

Figure 9. (A) HRTEM image of a thin, few-layer thick BN sheet taken from the edge of the thinnest BN flake (B) prepared by ultrasonication of a hexagonal BN crystal in dimethylformamide (DMF). The B−N bond distance is resolved, as pointed out in the sketch. (C) Bright spots on the HRTEM image show the center position of a six-membered B_3−N_3 hexagon (Golberg *et al.* 2010, unpublished data).

100 ms. However, a significant fraction within the yarns of BN phases other than tubes may be a concern.

Preparation of BN Nanosheets. Several years ago, BN nanosheets were first prepared by decomposition of borazine in the form of so-called nanomeshes on metallic substrates in the case of lattice mismatch, or on metal surfaces with a matching lattice,[103,104] and in folded shapes by solution[28] and/or ultrasonication[31] processing of a hexagonal BN. If there is no need for large quantities, such as for structural observations and/or the analysis of defect structures by HRTEM,[29,30,34] the BN flakes could be prepared nowadays by peeling using the Scotch adhesive tapes or chemical exfoliations of h-BN in ways similar to the graphene fabrications. Another approach designed in our group is mechanically assisted cleavage of BN flakes through ultrasonication, for example. The typical view of an individual BN nanosheet prepared by ultrasonication[31] of a hexagonal BN flake in dimethylformamide (DMF) is presented in Figure 9.

Properties of BNNTs. For many years, much interest has been devoted to bulky h-BN due to its low density, high thermal conductivity, electrical insulation, superb oxidation resistance, passivity to reactions with acids and melts, and low coefficient of friction. The BNNT, as an inheritor of the graphitic BN, takes all of these advantageous properties.

Compared with metallic or semiconducting CNTs, a BN nanotube is a wide band gap semiconductor with a band gap of *ca.* 5 eV.[11,12] Recent studies by Yap's group have pointed out a band gap of ~5.9 eV, approaching that of h-BN single crystals.[100,101] As mentioned in the previous sections, BNNTs have a rigid electronic structure, which is basically independent of the tube geometry/morphology. Along with the theoretical predictions discussed above,[54−60,64−66] BNNTs were indeed experimentally changed from insulators to narrow band n- or p-type semiconductors through doping,[105,106] deformation,[107] and/or functionalization.[108] Importantly, opposed to CNTs, BNNTs possess distinguishable chemical stability.[13] In fact, they are inert to most acids and alkalis. The thermal stability of BNNTs was confirmed using thermogravimetry (TG) analysis. While oxidation of standard CNTs already starts at *ca.* 450−500 °C, the reaction temperature of BNNTs with air shifts to a much higher temperature, *ca.* 950−1000 °C.[9,13,14] Thus, BNNTs are supposed to be more practical than CNTs for nanotube-based nanodevices or protective shields on various nanomaterials, especially for those performing at high temperatures and in hazardous environments.

CNTs are known to be excellent thermal conductors, and the thermal conductivity of BNNTs might be comparable to that of CNTs. The high thermal conductivity (k) on the order of 350 W mK^{-1} was experimentally confirmed at room temperature for isotopically enriched BNNTs having an outer diameter of 30−40 nm.[109] Furthermore, as for CNTs, the asymmetric axial thermal conductance properties of BNNTs homogeneously covered with heavy molecules were also found to be remarkable.[110]

Time-resolved photoluminescence spectroscopic studies were performed by Wu *et al.*[111] on the multiwalled BNNTs prepared using the CNT template method. Nanotubes were excited with a laser line at 267 nm. Photon replica-dominated luminescence band was observed from 295 to 350 nm. A comparison of the BNNTs' photoluminescence with that of hexagonal BN implied the existence of a spatially indirect band gap in the tubes. On the other hand, Jaffrennou *et al.*[112] performed cathodoluminescence (CL) imaging and low-temperature study on an individual multiwalled BNNT. The authors observed a strong broad-band emission centered at 320 nm (3.9 eV) and a weak peak centered at 233 nm (5.3 eV). The luminescence was located all

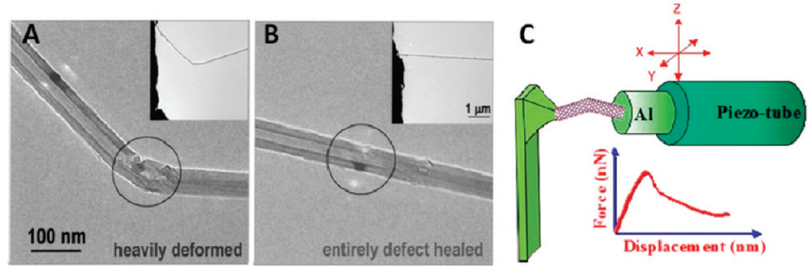

Figure 10. (A,B) HRTEM images of a multiwalled BN nanotube under its bending and reloading in the transmission electron microscope. The AFM-TEM holder setup is sketched in panel C. The tube fully restores its original shape due to unmatched elasticity and flexibility. No defects are left in the reloaded tube, despite severe tube shell corrugations at bending, as circled in panel A. The insets in panels A and B show the same tube at a lower magnification. The force−displacement curves (C) are recorded in tandem with the TEM imaging. (A,B) Adapted from ref 9.

along the nanotube. In comparison with the related bulk material, h-BN, the authors pointed out the strong luminescence recorded around ~230 nm. This was attributed to the excitonic effects, more precisely to excitons bound to the structural defects: dislocations and facets, which were indeed observed along the tube walls by HRTEM. The regarded two optical studies seem to contradict each other. This is due to the fact that some very important parameters related to the band/electronic structures of BNNTs and even bulk h-BN are still ambiguous (*e.g.*, the issues of direct/indirect band gaps, Wannier/Frenkel excitons, and the significance of one-dimensional (1D) quantum confinement effects have still been under debate). In spite of these questions, there has been a general agreement in the literature that BNNTs, similarly to h-BN,[113] may be an ideal candidate for optical nanodevices working in the UV regime. Moreover, the photoluminescence quantum yield of BNNTs was thought to surpass that of CNTs. In fact, intense and stable UV emission of BNNTs has been observed by Zhi *et al.*[114] and some other researchers.

Recent studies have indicated that BNNTs exhibit excellent elastic properties, and the mechanical stiffness of BNNTs rivals that of CNTs. In the pioneering work by Chopra and Zettl,[115] the Young modulus of BNNTs was measured to be *ca.* 1.1−1.3 TPa. Thus, BNNTs are possibly the stiffest insulating fibers ever known. In a more recent work by Golberg *et al.*,[36] direct bending force measurements were performed during deformation of multiwalled BNNTs of different diameters (40−100 nm) prepared *via* the BOCVD method using an AFM device integrated into a high-resolution TEM. BNNTs were found to be very flexible and entirely elastic under loading (Figure 10). The bending stress values of BNNTs were measured between ~100 and 260 MPa, and the elastic modulus of a BNNT was estimated to be 0.5−0.6 TPa. The bending deformation was proceeded by kinking, but not by arching/bowing as in a regular case of a cylinder-like CNT. The initial kinks did not appear in the middle tube zones; rather, they first formed at the tube sides close to the clamps. This is due to preexisting stress−strain fields within multilayered polygonal cross-sectional BN walls.

There have been many interesting physicochemical properties of BNNTs not discussed in this contribution due to space limitations. These include piezoelectricity,[116] immobilization of ferritin proteins on BNNT surfaces[117] for some prospective medical and nanobiological applications, irradiation stabilities of BNNTs, and so on. One can find many of these and other issues in our recent article.[9] It is worth noting that, although there is a vast interest in exploring the unique properties of BN tubes, so far, most of the experimentally evaluated properties were measured on multiwalled BNNTs with comparatively large diameters, *ca.* >10 nm. Such a situation partially results from the lack of ultrafine BNNTs (with diameters of a few nanometers, including SWNTs) of high quantity and quality and partially is due to many technical difficulties involved in testing of the smaller objects.

Properties and Applications of BN Nanosheets. The mechanical properties of BN nanosheets have recently been elucidated by our group.[33] The bending modulus was found to depend on the sheet thickness approaching the theoretical limit in the thinnest sheets, a few nanometers thick (Figure 11). These BN sheets were found to be quite useful for the reinforcement of polymeric films. The elastic modulus of PMMA (polymethyl methacrylate) films was increased by 22% and its strength by ~11% while incorporating only 0.3 wt % of BN nanosheets into the polymer.[31]

Prospective BN Nanotube Applications. The most logically expected application of BNNT stems from their superb thermal and oxidation stability and chemical inertness. They may be smartly used as protective capsules for any type of encapsulating nanomaterials, which otherwise would be not stable in air, and/or easily contaminated at ambient conditions. Figure 12 shows such a tubular BN capsule for very small catalytic Pt particles (with an average size of only ~2 nm). Applications of multiwalled BN tubes as protective shields/capsules for diverse functional materials, such as semiconducting nanowires,[118] magnetic nanorods,[119] and luminescent nanomaterials,[120] have indeed been reported.

Multiwalled BNNTs were also found to be valuable for the reinforcement[121] and/or increase in thermal

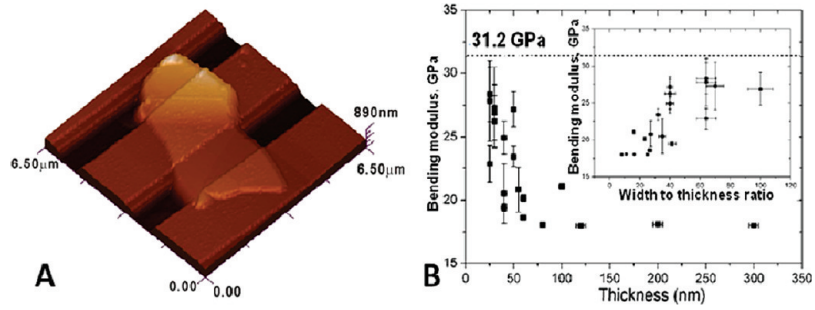

Figure 11. (A) AFM topography image of a Ti/Au contact-clamped BN nanosheet placed under the trench on a Si/SiO_2 substrate. (B) Measured bending modulus of BN nanosheets as a function of their dimensions. Adapted from ref 33.

conductivity[122,123] of insulating polymeric films and fibers. The yield stress and/or elastic modulus of insulating polymer films may be increased 30−50% by loading with rather modest weight fractions of BNNTs, only 1−3%.[121] Figure 13A shows a macrofilm (5 cm × 5 cm) made of numerous stacked BNNTs-containing PVA (polyvinyl alcohol) sheets. The sheets were made by merging aligned electrospinned polymeric fibers loaded with 10 wt % of BNNTs.[123] Importantly, the BNNT axes were also aligned along the fiber axes during electrospinning. The image in Figure 13B shows the same film after hot-pressing at 90 °C. The film becomes fully transparent due to a complete dissolution of polymeric fibers. BNNTs do not change either their alignment within the macrofilm or morphology/structure at such moderate temperature treatment and remained assembled in parallel within the film. Since the tubes do not absorb a visible light due to a wide band gap (~5.5 eV), the film is entirely transparent. The thermal conductivity of such film was increased more than 3-fold, from ~0.16 to ~0.54 W/mK due to the effect of BNNTs when measured along the aligned BNNTs' axes direction.

BNNTs can also be decent field emitters and pH sensors. Very recently, the submicrometer-sized sensors were fabricated out of biotin−fluorescein-functionalized multiwalled BN nanotubes with anchored Ag nanoparticles (Figure 14).[124] Intrinsic pH-dependent photoluminescence and Raman signals in attached fluorescein molecules enhanced by surface-enhanced resonance on decorated Ag nanoparticles (~20 nm in size) allow these novel nanohybrids to perform as practical three-dimensional pH mapping probes. The spatial resolution of the pH measurements was determined by a laser spot size and a BNNT diameter. Using the calibrated pH/Raman intensity ratio curves, the environmental pH values of subunits in living cells (where a traditional optical fiber sensor fails because of spatial limitations) could be determined. If one can fix a Raman laser spot on a specific site on a hybrid BN nanotube and assemble the tubes into a robotic control system, the probe should detect the pH values in any position one is interested in, without the necessity to fill other labels.

Yap's group found that the BNNT nanotube films are superhydophobic[125] (Figure 15). The effect may be smartly used in making not wetting and/or self-cleaning glasses and windows. Interestingly, such hydrophobicity is in striking contrast with the standard BN thin film behavior which can be partially wetted by water.

Recently, it was theoretically demonstrated that single-walled BN nanotubes have the ability to carry out some of the important functions of biological ion channels.[126] The tubes with radii of 4.83 and 5.52 Å embedded in a silicon nitride membrane were selectively permeable to cations and anions, respectively. The

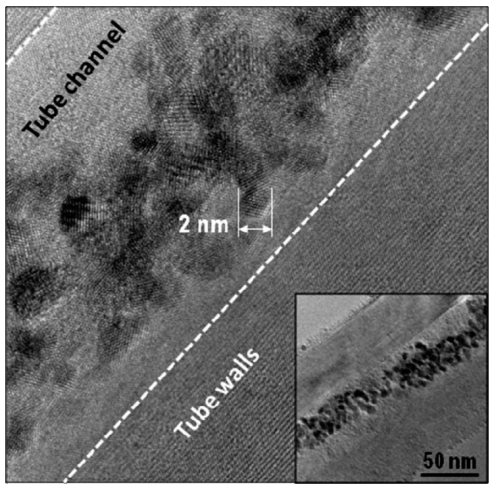

Figure 12. HRTEM image of a multiwalled BNNT capsule/container. Numerous tiny platinum particles (~2 nm in diameter) are encapsulated and sealed in it, providing their entire protection from oxidation/contamination (Golberg *et al.* 2010, unpublished results).

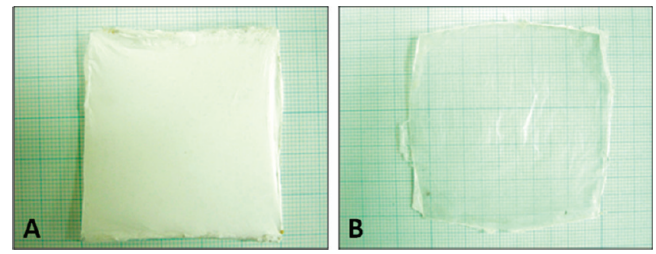

Figure 13. (A) PVA macrosheet (~5 cm × 5 cm in size) made of 18 stacked plates with aligned PVA fibers (each loaded with 10 wt % of BNNTs). (B) Same sheet after hot-pressing at 90 °C; it becomes fully transparent because of fiber dissolution and revealed more than a 3-fold increase in thermal conductivity due to the positive effect of dissolved and ultimately aligned highly thermoconductive BN tubes in a polymer matrix.

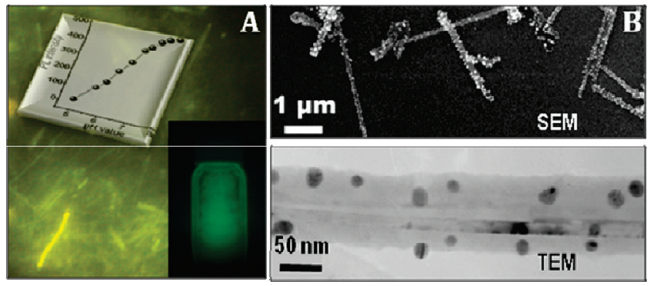

Figure 14. (A) Diagram showing pH-dependent fluorescence intensity of a multiwalled BNNT−biotin−Ag nanoparticle hybrid and an optical image of fluorescent BNNT tubes. The inset in panel A is an image of a hybrid BN nanotube powder under 325 nm UV light illumination. (B) Low- and high-magnification TEM images of biotin−fluorescein-functionalized BNNTs with decorated Ag nanoparticles (B). Adapted from ref 124.

tubes mimic some of the permeation characteristics of gramicidin and chloride channels. Such tiny tubes were suggested to have potential applications as sensitive biosensors, antibiotics, or filtration devices. The same group[127] has computed that SWNT BN nanotubes show superior water flow properties compared to CNTs and are thus expected to provide a more efficient water purification device. Using molecular dynamics simulations, the authors showed that a (5,5) arm-chair BN nanotube in a Si nitride membrane can obtain 100% salt rejection at concentrations as high as 1 M owing to a high energy barrier while still allowing water molecules to flow at a rate as high as 10.7 water molecules/ns, or 0.9268 L m^{-2} h^{-1}.

Although several biomedical applications of CNTs have already been proposed, the use of BNNTs in this field has largely been unexplored. Ciofani *et al.*[128] have initiated an experimental program aimed at the exploration of the interactions between multiwalled BNNTs and living cells. The authors reported on the magnetic properties of BNNTs with Fe catalysts and confirmed the feasibility for their use as nanovectors for targeted drug delivery. *In vitro* tests have shown a dependence of the BNNT uptake by living cells on exposure to an external magnetic source. Following this work, Huang *et al.*[129] have also shown that multiwalled BNNTs can become fully magneto-operable under their surface functionalization with Fe_3O_4 superparamagnetic nanoparticles.

Through first-principles electron dynamic simulations under applied fields, Yan *et al.*[130] have confirmed

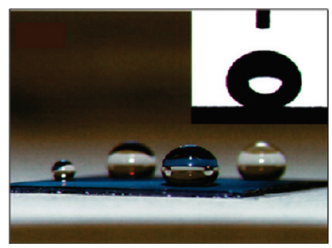

Figure 15. Photograph of water droplets on a film made of short multiwalled BN nanotubes showing superhydrophobicity. Adapted from ref 125.

that the alkali-doped BNNTs can generate an emission current 2 orders of magnitude larger than CNTs. The nodeless wave function at the Fermi level, together with the lowered work function, constitutes the major advantage of the alkali-doped BNNTs. The authors proposed that such a doped BNNT should be an excellent electron emitter in terms of the large emission current as well as its chemical and mechanical stability. In fact, we observed the decent field emission even from undoped multiwalled BNNTs several years ago.[131]

Alkali metal atoms and alkaline-earth metal ions inserted into a single-walled BNNT have recently become of interest from a perspective of quantum computing.[132] Theoretically, it was shown that the spin density is localized on intercalated individual alkali atoms or ions. The antiferromagnetic state of a linear chain of such atoms and ions is energetically more favorable. However, the exchange interaction between spins is fairly weak. Therefore, such BN tube-based systems were suggested to be used as two qubit cells for a quantum computer.

Other prospective applications of BN nanotubes, which include gas adsorbents, spintronic devices, UV lasers, high resistivity substrates ($R > 10$ GΩ), and interconnects for nanoscale electronics, radiation stoppers, and reinforcing agents for functional airspace metals/ceramics, are also on the agenda. These deserve further studies and developments.[9]

Conclusion and Perspective. In spite of the promising future of BN nanotubes and BN nanosheets, the progress in their research has been rather marginal to date, especially when compared to that of CNTs and graphenes (Figure 2). It is suggested that such a situation is primarily the result of significant difficulties involved in the BN nanophase preparations. To date, various synthetic methods for BNNTs and nanosheets have been developed; however, the yield and/or purity of the products is still far from satisfactory and is not enough for the immediate commercialization. By using the BOCVD method,[93,94] large-scale synthesis of pure multiwalled BNNTs has already been achieved. Some novel methods have also displayed promise.[90] However, up to now, BNNTs synthesized *via* most of the existing routes have relatively large diameters of ~50 nm. There is still a challenge in finding a way to finely control/downsize the tube diameters using any method. In fact, some functional properties and particularly a defect structure of BNNTs may have a close relationship with their diameters and morphologies. Thus, present lacking of the structural diversity surely limits the new property investigations and applications of BNNTs. Synthetic research on BN nanosheets is still in its embryo stage, and very few works related to their synthesis and property investigations have been published to date.[27−35]

On the other hand, a key feature that has attracted much research effort with respect to conventional C nanotubes is the ability of their surfaces to be chemi-

cally functionalized. It has allowed the solubilization of nanotubes/nanosheets in a given solvent, the integration into host materials to form composites, and the assembly with diverse nanomaterials. In particular, the combination of nanoparticles and CNTs was an interesting approach: on one hand, CNTs can be a support for nanoparticles, and on the other hand, nanoparticles can widen the range of tube properties. In recent years, studies on the analogous functionalization of BNNTs have also been initiated. Several kinds of nanoparticles, such as Au, Ag,[124] and SnO_2,[133] were functionalized on BNNT surfaces to form BNNT-based nanocomposites. However, compared to CNTs, the research on BNNT-based nanocomposites with foreign inorganic nanoparticles has had relatively modest progress. No experimental data have been published with respect to BN nanosheet chemical modifications. That is partially due to the lacking of the effective methods to prepare BN nanotubes and nanosheets on a large scale. Another reason is that BN nanostructures possess high chemical stability and poor wetting properties at ambient conditions, which make direct and uniform coatings/functionalizations difficult. Developing an effective method to achieve surface functionalization of BN tubes/sheets with diverse nanoparticles and/or functional substances is thus highly desirable.

Before real integration of BN nanotubes/nanosheets into modern nanotechnology in order to meet the human needs, the key targets at present are on-demand nanomaterial physical and chemical manipulations, as well as their novel physicochemical property assessments toward prospective applications. The BN nanotubes seem to be nontoxic.[134,135] This is a solid advantage of these nanomaterials as far as transparent and safe practical applications are concerned. Needless to say, nontoxity of BN tubes/sheets has to be reconfirmed in numerous tests and under varying experimental conditions before the BNNT-based products may go into the market.

Structural resemblance between C and BN nanoscale systems gives an excellent match between the two in many prospective applications. The C−BN heterostructures may be interesting in synthetic,[136−138] electronic,[139−141] and magnetic applications.[142,143] As C nanostructures are metallic or semiconducting, whereas those of BN are electrically insulating, the BN nanomaterials are able to nicely serve as atomically compatible insulating substrates in electrical applications of CNTs and graphenes, preventing current leakage and short currents. Prior to this, stability of BN nanostructures under high current densities should be thoroughly elucidated.[144,145]

Along with the developments of synthetic methods, the analytical tools to precisely resolve the atomic and defect structure of BN nanotubes and nanosheets aimed at the clear understanding of structure−property relationships need to be developed. For example, recent breakthroughs in analytical transmission electron microscopy toward atom-by-atom structural and chemical analysis of BN monatomic sheets have nicely been demonstrated by Krivanek *et al*.[146] The authors have been able to determine three types of atomic substitutions, namely, C for B, C for N, and O for N in a monolayer BN sheet using an annular dark-field technique and an aberration-corrected transmission electron microscope.

By taking into account all of the above-mentioned and pre-existing restrictions/limitations of the BN nanotube/nanosheet syntheses and analyses, their modifications, and practical utilizations, the scientists should now focus on a design of the tube diameter and sheet thickness controllable syntheses and targeted surface functionalizations of BN nanostructures. The final goal of these efforts is the detailed evaluation of their advanced properties required for future high-performance composites, nano-, bio-, electromechanical, and medical devices.

Acknowledgment. The authors acknowledge financial support of the International Center for Materials Nanoarchitectonics (MANA) of the National Institute for Materials Science (NIMS), Tsukuba, Japan. The authors are indebted to Akihiko Nukui, Isamu Yamada, and Keiji Kurashima for continuous technical support.

REFERENCES AND NOTES

1. Oberlin, A.; Endo, M.; Koyama, T. Filamentous Growth of Carbon through Benzene Decomposition. *J. Cryst. Growth* **1976**, *32*, 335–349.
2. Iijima, S. Helical Microtubules of Graphitic Carbon. *Nature* **1991**, *354*, 56–58.
3. Ishii, T.; Sato, T.; Sekikawa, Y.; Iwata, M. Growth of Whiskers of Hexagonal Boron Nitride. *J. Cryst. Growth* **1981**, *52*, 285–289.
4. Paine, R. T.; Narula, C. K. Synthetic Routes to Boron Nitride. *Chem. Rev.* **1990**, *90*, 73–91.
5. Chopra, N. G.; Luyken, R. J.; Cherrey, K.; Crespi, V. H.; Cohen, M. L.; Louie, S. G.; Zettl, A. Boron Nitride Nanotubes. *Science* **1995**, *269*, 966–967.
6. Loiseau, A.; Willaime, F.; Demoncy, N.; Hug, G.; Pascard, H. Boron Nitride Nanotubes with Reduced Numbers of Layers Synthesized by Arc Discharge. *Phys. Rev. Lett.* **1996**, *76*, 4737–4740.
7. Terrones, M.; Hsu, W. K.; Terrones, H.; Zhang, J. P.; Ramos, S.; Hare, J. P.; Castillo, R.; Prassides, K.; Cheetham, A. K.; Kroto, H.; *et al.* Metal Particle Catalysed Production of Nanoscale BN Structures. *Chem. Phys. Lett.* **1996**, *259*, 568–573.
8. Golberg, D.; Bando, Y.; Eremets, M.; Takemura, K.; Kurashima, K.; Yusa, H. Nanotubes in Boron Nitride Laser Heated at High Pressure. *Appl. Phys. Lett.* **1996**, *69*, 2045–2047.
9. Golberg, D.; Bando, Y.; Tang, C. C.; Zhi, C. Y. Boron Nitride Nanotubes. *Adv. Mater.* **2007**, *19*, 2413–2432.
10. Novoselov, K. S.; Geim, A. K.; Morozov, S. V.; Jiang, D.; Zhang, Y.; Dubonos, S. V.; Grigorieva, I. V.; Firsov, A. A. Electric Field Effect in Atomically Thin Carbon Films. *Science* **2004**, *306*, 666–669.
11. Rubio, A.; Corkill, J. L.; Cohen, M. Theory of Graphitic Boron Nitride Nanotubes. *Phys. Rev. B* **1994**, *49*, 5081–5084.
12. Blase, X.; Rubio, A.; Louie, S. G.; Cohen, M. L. Stability and Band-Gap Constancy of Boron-Nitride Nanotubes. *Europhys. Lett.* **1994**, *28*, 335–340.

13. Golberg, D.; Bando, Y.; Kurashima, K.; Sato, T. Synthesis and Characterization of Boron Nitride Multiwalled Nanotube Ropes. *Scr. Mater.* **2001**, *44*, 1561–1564.
14. Chen, Y.; Zou, J.; Campbell, S. J.; Caer, G. L. Boron Nitride Nanotubes: Pronounced Resistance to Oxidation. *Appl. Phys. Lett.* **2004**, *84*, 2430–2432.
15. Arenal, R.; Ferrari, A. C.; Reich, S.; Wirtz, L.; Mevellec, J. Y.; Lefrant, S.; Rubio, A.; Loiseau, A. Raman Spectroscopy of Single-Wall Boron Nitride Nanotubes. *Nano Lett.* **2006**, *6*, 1812–1816.
16. Andujar, J. L.; Bertran, E.; Maniette, Y. Microstructure of Highly Oriented, Hexagonal, Boron Nitride Thin Films Grown on Crystalline Silicon by Radio Frequency Plasma-Assisted Chemical Vapor Deposition. *J. Appl. Phys.* **1996**, *80*, 6553–6555.
17. Huang, J. L.; Pan, C. H.; Lii, D. F. Investigation of the BN Films Prepared by Low Pressure Chemical Vapor Deposition. *Surf. Coat. Technol.* **1999**, *122*, 166–175.
18. Choi, B. J. Chemical Vapor Deposition of Hexagonal Boron Nitride Films in the Reduced Pressure. *Mater. Res. Bull.* **1999**, *34*, 2215–2220.
19. El-Yadouni, A.; Soltani, A.; Boudrioua, A.; Thevenin, P.; Bath, A.; Loulergue, J. C. Investigation of the Optical and Electro-Optical Properties of Hexagonal Boron Nitride Thin Films Deposited by PECVD Technique. *Opt. Mater.* **2001**, *17*, 319–322.
20. Kalss, W.; Haubner, R.; Lux, B. Preparation of BN Films in the B−N−F System. *Diamond Relat. Mater.* **1998**, *7*, 369–375.
21. Zhang, W. J.; Matsumoto, S. The Roles of Hydrogen and Fluorine in the Deposition of Cubic Boron Nitride Films in the Ar−N2−BF3−H2 System. *Chem. Phys. Lett.* **2000**, *330*, 243–248.
22. Zhang, W. J.; Chan, C. Y.; Meng, X. M.; Fung, M. K.; Bello, I.; Lifshitz, Y.; Lee, S. T.; Jiang, X. The Mechanism of Chemical Vapor Deposition of Cubic Boron Nitride Films from Fluorine-Containing Species. *Angew. Chem., Int. Ed.* **2005**, *44*, 4749–4753.
23. Zhang, W. J.; Matsumoto, S. The Effects of DC Bias Voltage on the Crystal Size and Crystal Quality of cBN Films. *Appl. Phys. A: Mater. Sci. Process.* **2000**, *71*, 469–472.
24. Yu, J.; Zheng, Z.; Ong, H. C.; Wong, K. Y.; Matsumoto, S.; Lau, W. M. Thermal Stability of Cubic Boron Nitride Films Deposited by Chemical Vapor Deposition. *J. Phys. Chem. B* **2006**, *110*, 21073–21076.
25. Matsumoto, S.; Nishida, N.; Akashi, K.; Sugai, K. Preparation of BN Films by RF Thermal Plasma Chemical Vapour Deposition. *J. Mater. Sci.* **1996**, *31*, 713–720.
26. Mirkarimi, P. B.; McCarty, K. F.; Medlin, D. L. Review of Advances in Cubic Boron Nitride Film Synthesis. *Mater. Sci. Eng. Rev.* **1997**, *21*, 47−100, and references therein.
27. Zhu, Y. C.; Bando, Y.; Yin, L. W.; Golberg, D. Field Nanoemitters: Ultrathin BN Nanosheets Protruding from Si_3N_4 Nanowires. *Nano Lett.* **2006**, *6*, 2982–2986.
28. Han, W. Q.; Wu, L. J.; Zhu, Y. M.; Watanabe, K.; Taniguchi, T. Structure of Chemically Derived Mono- and Few-Atomic-Layer Boron Nitride Sheets. *Appl. Phys. Lett.* **2008**, *93*, 223103.
29. Pacile, D.; Meyer, J. C.; Girit, C. O.; Zettl, A. The Two-Dimensional Phase of Boron Nitride: Few-Atomic-Layer Sheets and Suspended Membranes. *Appl. Phys. Lett.* **2008**, *92*, 133107.
30. Alem, N.; Erni, R.; Kiselowski, C.; Rossell, M. D.; Gannett, W.; Zettl, A. Atomically Thin Hexagonal Boron Nitride Probed by Ultrahigh-Resolution Transmission Electron Microscopy. *Phys. Rev. B* **2009**, *80*, 155425.
31. Zhi, C. Y.; Bando, Y.; Tang, C. C.; Kuwahara, H.; Golberg, D. Large-Scale Fabrication of Boron Nitride Nanosheets and Their Utilization in Polymeric Composites with Improved Thermal and Mechanical Properties. *Adv. Mater.* **2009**, *21*, 2889–2893.
32. Gao, R.; Yin, L. W.; Wang, C. X.; Qi, Y. X.; Lun, N.; Zhang, L.; Liu, Y. X.; Kang, L.; Wang, X. F. High-Yield Synthesis of Boron Nitride Nanosheets with Strong Ultraviolet Cathodoluminescence Emission. *J. Phys. Chem. C* **2009**, *113*, 15160–15165.
33. Li, C.; Bando, Y.; Zhi, C. Y.; Huang, Y.; Golberg, D. Thickness Dependent Bending Modulus of Hexagonal Boron Nitride Nanosheets. *Nanotechnology* **2009**, *20*, 385707.
34. Warner, J. H.; Rummeli, M. H.; Bachmatiuk, A.; Buchner, B. Atomic Resolution Imaging and Topogarphy of Boron Nitride Sheet Produced by Chemical Exfoliation. *ACS Nano* **2010**, *4*, 1299–1304.
35. Nag, A; Raindogia, K.; Hembram, K. P. S. S.; Datta, R; Wangmare, U. V.; Rao, C. N. R. Graphene Analogues of BN: Novel Synthesis and Properties. *ACS Nano* **2010**, *4*, 1539–1544.
36. Golberg, D.; Costa, P. M. F. J.; Lourie, O.; Mitome, M.; Tang, C.; Zhi, C. Y.; Kurashima, K.; Bando, Y. Direct Force Measurements and Kinking under Elastic Deformation of Individual Multiwalled Boron Nitride Nanotubes. *Nano Lett.* **2007**, *7*, 2146–2151.
37. Celik-Atkas, A.; Zuo, J. M.; Stubbins, J. F.; Tang, C.; Bando, Y. Double-Helix Structure in Multiwall Boron Nitride Nanotubes. *Acta Crystallogr., Sect. A* **2005**, *61*, 533–541.
38. Golberg, D.; Mitome, M.; Bando, Y.; Tang, C. C.; Zhi, C. Y. Multi-Walled Boron Nitride Nanotubes Composed of Diverse Cross-Section and Helix Type Shells. *Appl. Phys. A: Mater. Sci. Process.* **2007**, *88*, 347–352.
39. Tibbets, K.; Doe, R.; Ceder, G. Polygonal Model for Layered Inorganic Nanotubes. *Phys. Rev. B* **2009**, *80*, 014102.
40. Saito, Y.; Maida, M.; Matsumoto, T. Structures of Boron Nitride Nanotubes with Single-Layer and Multilayers Produced by Arc-Discharge. *Jpn. J. Appl. Phys.* **1999**, *38*, 159–163.
41. Golberg, D.; Bando, Y.; Kurashima, K.; Sato, T. Ropes of BN Multi-Walled Nanotubes. *Solid State Commun.* **2000**, *116*, 1–7.
42. Kim, Y.-H.; Chang, K. J.; Louie, S. G. Electronic Structure of Radially Deformed BN and BC_3 Nanotubes. *Phys. Rev. B* **2001**, *63*, 205408.
43. Barnard, A. S.; Snook, I. K.; Russo, S. P. Bonding and Structure in B_xN_y Nanotubes ($x,y = 1,2$). *J. Mater. Chem.* **2007**, *17*, 2892–2898.
44. Guo, G. Y.; Ichihashi, S.; Tamura, T.; Terakura, K. Static Dielectric Response and Born Effective Charge of BN Nanotubes from *Ab Initio* Finite Electric Field Calculations. *Phys. Rev. B* **2007**, *75*, 245403.
45. Chou, Y. M.; Wang, H. W.; Lin, Y. J.; Chen, W. H.; Wang, B. C. Infinite Single-Walled Boron-Nitride Nanotubes Studied by LGTO-PBC-DFT Method. *Diamond Relat. Mater.* **2009**, *18*, 351–354.
46. Li, X. M.; Tian, W. Q.; Huang, X. R.; Sun, C. C.; Jiang, L. Theoretical Exploration of the Armchair BN Nanotube with Defects. *J. Nanopart. Res.* **2009**, *11*, 395–403.
47. Chen, C. W.; Lee, M. H.; Clark, S. J. Band Gap Modification of Single-Walled Carbon Nanotube and Boron Nitride Nanotube under a Transverse Electric Field. *Nanotechnology* **2004**, *15*, 1837.
48. Guo, J. G.; Zhi, C. Y.; Wang, E. G. Boron Carbonitride Nanojunctions. *Appl. Phys. Lett.* **2002**, *80*, 124–126.
49. Attaccalite, C.; Wirtz, L.; Mirini, A.; Rubio, A. Absorption of BN Nanotubes under the Influence of a Perpendicular Electric Field. *Phys. Status Solidi* **2007**, *244*, 4288–4292.
50. Hu, S. L.; Li, Z. Y.; Zeng, X. C.; Yang, J. L. Electronic Structure of Defective Boron Nitride Nanotubes under Transverse Electric Field. *J. Phys. Chem. C* **2008**, *112*, 8424–8428.
51. Khoo, K. H.; Mazzoni, M. S. C.; Louie, S. G. Tuning the Electronic Properties of Boron Nitride Nanotubes with Transverse Electric Fields: A Giant DC Stark Effect. *Phys. Rev. B* **2004**, *69*, 201401.
52. Park, C. H.; Louie, S. G. Energy Gaps and Stark Effect in Boron Nitride Nanoribbons. *Nano Lett.* **2008**, *8*, 2200–2203.
53. Lan, H. P.; Ye, L. H.; Zhang, S. A.; Peng, L. M. Transverse Dielectric Properties of Boron Nitride Nanotubes by *Ab Initio* Electric Field Calculations. *Appl. Phys. Lett.* **2009**, *94*, 183110.

54. Zheng, F. W.; Zhou, G.; Hao, S. G.; Duan, W. H. Structural Characterization and Electronic Properties of Boron Nitride Crystalline Bundles. *J. Chem. Phys.* **2005**, *123*, 124716.
55. Wang, Z. G.; Li, Z.; Cheng, D. M. Effects of Uniaxial Strain on the Band Structure of Boron Nitride Nanotubes: A First Principle Study. *Eur. Phys. J* **2009**, *69*, 20601.
56. Guerini, S.; Kar, T.; Piquini, P. Theoretical Study of Si Impurities in BN Nanotubes. *Eur. Phys. J. B* **2004**, *38*, 515–518.
57. Zhang, J.; Loh, K. P.; Yang, S. W.; Wu, P. Exohedral Doping of Single-Walled Boron Nitride Nanotubes by Atomic Chemisorption. *Appl. Phys. Lett.* **2005**, *87*, 243105.
58. Yan, B.; Park, C.; Ihm, J.; Zhou, G.; Duan, W.; Park, N. Electron Emission Originated from Free-Electron-like States of Alkali-Doped Boron-Nitride Nanotubes. *J. Am. Chem. Soc.* **2008**, *130*, 17012–17015.
59. Cho, Y. J.; Kim, C. H.; Kim, H. S.; Park, J.; Choi, H. C.; Shin, H. J.; Gao, G.; Kang, H. S. Electronic Structure of Si-Doped BN Nanotubes Using X-ray Photoelectron Spectroscopy and First Principles Calculations. *Chem. Mater.* **2009**, *21*, 136–143.
60. Gou, G. Y.; Pan, B. C.; Shi, L. The Nature of Radiative Transitions in O-Doped Boron Nitride Nanotubes. *J. Am. Chem. Soc.* **2009**, *131*, 4839–4845.
61. Schmidt, T. M.; Baierle, R. J.; Piquini, P.; Fazzio, A. Theoretical Study of Native Defects in BN Nanotubes. *Phys. Rev. B* **2003**, *67*, 113407.
62. An, W.; Wu, X. J.; Yang, J. L.; Zeng, X. C. Adsorption and Surface Reactivity on Single-Walled Boron Nitride Nanotubes Containing Stone-Wales Defects. *J. Phys. Chem. C* **2007**, *111*, 14105–14112.
63. Li, Y. F.; Zhou, Z.; Golberg, D.; Bando, Y.; Schleyer, P. V.; Chen, Z. F. Stone-Wales Defects in Single-Walled Boron Nitride Nanotubes: Formation Energies, Electronic Structures, and Reactivity. *J. Phys. Chem. C* **2008**, *112*, 1365–1370.
64. Wu, X. J.; Yang, J. L.; Zeng, X. C. Adsorption of Hydrogen Molecules on the Platinum-Doped Boron Nitride Nanotubes. *J. Chem. Phys.* **2006**, *125*, 044704.
65. Wang, R. X.; Zhu, R. X.; Zhang, D. J. Adsorption of Fomaldehyde Molecule on the Pristine and Silicon Doped Boron Nitride Nanotubes. *Chem. Phys. Lett.* **2008**, *467*, 131–135.
66. Zhang, Z. H.; Guo, W. L. Tunable Ferromagnetic Spin Ordering in Boron Nitride Nanotubes with Topological Fluorine Adsorption. *J. Am. Chem. Soc.* **2009**, *131*, 6874–6879.
67. Zhou, Z.; Zhao, J. J.; Chen, Z. F.; Schleyer, P. V. Atomic and Electronic Structures of Fluorinated BN Nanotubes: Computational Study. *J. Phys. Chem. B* **2006**, *110*, 25678–25685.
68. Zhang, J.; Loh, K. P.; Wu, P.; Sullivan, M. B.; Zheng, J. W. Chemisorption-Induced Polarization of Boron Nitride Nanotubes. *J. Phys. Chem. C* **2008**, *112*, 10279–10286.
69. Li, J.; Zhou, G.; Chen, Y.; Gu, B.-L.; Duan, W. H. Magnetism of C Adatoms on BN Nanostuctures: Implications for Functional Nanodevices. *J. Am. Chem. Soc.* **2009**, *131*, 1796–1801.
70. Okada, S.; Saito, S.; Oshiyama, A. Interwall Interaction and Electronic Structure of Double-Walled BN Nanotubes. *Phys. Rev. B* **2002**, *65*, 165410.
71. Jhi, S. H.; Roundy, D. J.; Louie, S. G.; Cohen, M. L. Formation and Electronic Properties of Double-Walled Boron Nitride Nanotubes. *Solid State Commun.* **2005**, *134*, 397–402.
72. Liu, H. T.; Zhou, G.; Yan, Q. M.; Wu, J.; Gu, B. L.; Duan, W. H.; Zhao, D. L. Structural and Electronic Properties of Fluorinated Double-Walled Boron Nitride Nanotubes: Effect of Interwall Interaction. *Phys. Rev. B* **2007**, *75*, 125410.
73. Wirtz, L.; Marini, A.; Rubio, A. P. Excitons in Boron Nitride Nanotubes: Dimensionality Effects. *Phys. Rev. Lett.* **2006**, *96*, 126104.
74. Park, C. H.; Spataru, C. D.; Louie, S. G. Excitons and Many-Electron Effects in the Optical Response of Single-Walled Boron Nitride Nanotubes. *Phys. Rev. Lett.* **2006**, *96*, 126105.
75. Xu, Y. N.; Ching, W. Y. Calculation of Ground-State and Optical Properties of Boron Nitrides in the Hexagonal, Cubic, and Wurtzite Structures. *Phys. Rev. B* **1991**, *44*, 7787–7798.
76. Si, M. S.; Xue, D. S. Magnetic Properties of Vacancies in a Graphitic Boron Nitride Sheet by First-Principles Calculations. *Phys. Rev. B* **2007**, *75*, 193409.
77. Si, M. S.; Li, J. Y.; Shi, H. G.; Niu, X. N.; Xue, D. S. Divacancies in Graphitic Boron Nitride Sheets. *Eur. Phys. Lett.* **2009**, *86*, 46002.
78. Azevedo, S.; Kaschny, J. R.; de Castilho, C. M. C.; de Brito Mota, F. A Theoretical Investigation of Defects in a Boron Nitride Monolayer. *Nanotechnology* **2007**, *18*, 495707.
79. Terrones, M; Charlier, J.-C; Gloter, A; Cruz-Silva, E; Terrés, E; Li, Y. B.; Vinu, A; Dominguez, J. M.; Terrones, H; Bando, Y.; *et al.* Experimental and Theoretical Studies Suggesting the Possibility of Metallic Boron Nitride Edges in Porous Nanourchins. *Nano Lett.* **2008**, *8*, 1026–1032.
80. Yu, D. P.; Sun, X. S.; Lee, C. S.; Bello, I.; Lee, S. T.; Gu, H. D.; Leung, K. M.; Zhou, G. W.; Dong, Z. F.; Zhang, Z. Synthesis of Boron Nitride Nanotubes by Means of Excimer Laser Ablation at High Temperature. *Appl. Phys. Lett.* **1998**, *72*, 1966–1968.
81. Laude, T.; Matsui, Y.; Marraud, A.; Joufrey, B. Long Ropes of Boron Nitride Nanotubes Grown by a Continuous Laser Ablation. *Appl. Phys. Lett.* **2000**, *76*, 3239–3241.
82. Arenal, R.; Stephan, O.; Cochon, J.; Loiseau, A. Root-Growth Mechanism of Single-Walled Boron Nitride Nanotubes *via* Laser Vaporization Technique. *J. Am. Chem. Soc.* **2007**, *129*, 16183–16189.
83. Chen, Y.; Chadderton, L. T.; FitzGerald, J.; Williams, J. S.; Bulcock, S. A Solid State Process for Formation of Boron Nitride Nanotubes. *Appl. Phys. Lett.* **1999**, *74*, 2960–2962.
84. Lourie, O. R.; Jones, C. R.; Bartlett, B. M.; Gibbons, P. C.; Ruoff, R. S.; Buhro, W. E. CVD Growth of Boron Nitride Nanotubes. *Chem. Mater.* **2000**, *12*, 1808–1814.
85. Han, W. Q.; Bando, Y.; Kurashima, K.; Sato, T. Synthesis of Boron Nitride Nanotubes from Carbon Nanotubes by a Substitution Reaction. *Appl. Phys. Lett.* **1998**, *73*, 3085–3087.
86. Ma, R.; Bando, Y.; Sato, T.; Kurashima, K. Growth, Morphology and Structure of Boron Nitride Nanotubes. *Chem. Mater.* **2001**, *12*, 2965–2971.
87. Wang, J. S.; Kayastha, V. K.; Yap, Y. K.; Fan, Z. Y.; Lu, J. G.; Pan, Z. W.; Ivanov, I. N.; Puretzky, A. A.; Geohegan, D. B. Low Temperature Growth of Boron Nitride Nanotubes on Substrates. *Nano Lett.* **2005**, *5*, 2528–2532.
88. Nishiwaki, A.; Oku, T. Atomic Structures and Formation Mechanism of Boron Nitride Nanotubes and Nanohorns Synthesized by Arc-Melting LaB_6 Powders. *J. Eur. Ceram. Soc.* **2006**, *26*, 435–441.
89. Bourgeois, L.; Bando, Y.; Sato, T. Tubes of Rhombohedral Boron Nitride. *J. Phys. D: Appl. Phys.* **2000**, *33*, 1902–1908.
90. Smith, M. W.; Jordan, K. C.; Park, C.; Kim, J.-W.; Lillehei, P. T.; Crooks, R.; Harrison, J. S. Very Long Single- and Few-Walled Boron Nitride Nanotubes *via* the Pressurized Vapor/Condenser Method. *Nanotechnology* **2009**, *20*, 505604.
91. Altoe, M. V. P.; Sprunck, J. P.; Gabriel, J. C. P.; Bradley, K. Nanococoon Seeds for BN Nanotube Growth. *J. Mater. Sci.* **2003**, *38*, 4805–4810.
92. Kim, M. J.; Chatterjee, S.; Kim, S. M.; Stach, E. A.; Bradley, M. G.; Pender, M. J.; Sneddon, L. G.; Maruyama, B. Double-Walled Boron Nitride Nanotubes Grown by Floating Catalyst Chemical Vapor Deposition. *Nano Lett.* **2008**, *8*, 3298–3302.
93. Tang, C.; Bando, Y.; Sato, T.; Kurashima, K. A Novel Precursor for Synthesis of Pure Boron Nitride Nanotubes. *Chem. Commun.* **2002**, 1290–1292.
94. Zhi, C. Y.; Bando, Y.; Tang, C.; Golberg, D. Effective Precursor for High Yield Synthesis of Pure BN Nanotubes. *Solid State Commun.* **2005**, *135*, 67–70.
95. Golberg, D.; Bando, Y.; Kurashima, K.; Sato, T. MoO_3-Promoted Synthesis of Multi-Walled BN Nanotubes from C

Nanotube Templates. *Chem. Phys. Lett.* **2000**, *323*, 185–191.
96. Bechelany, M.; Bernard, S.; Brioude, A.; Cornu, D.; Stadelmann, P.; Charcosset, C.; Fiaty, K.; Miele, P. Synthesis of Boron Nitride Nanotubes by a Template-Assisted Polymer Thermolysis Process. *J. Phys. Chem. C* **2007**, *111*, 13378–13384.
97. Chen, H.; Chen, Y.; Liu, Y.; Fu, L.; Huang, C.; Lewellyn, D. Over 1.0 mm-Long Boron Nitride Nanotubes. *Chem. Phys. Lett.* **2008**, *463*, 130–133.
98. Li, Y.; Zhou, J.; Zhao, K.; Tung, S.; Schneider, E. Synthesis of Boron Nitride Nanotubes from Boron Oxide by Ball Milling and Annealing Process. *Mater. Lett.* **2009**, *63*, 1733–1736.
99. Singhal, S. K.; Srivastava, A. K.; Pant, R. P.; Halder, S. K.; Singh, B. P.; Gupta, A. K. Synthesis of Boron Nitride Nanotubes Employing Mechanothermal Process and Its Characterization. *J. Mater. Sci.* **2008**, *43*, 5243–5250.
100. Lee, C. H.; Xie, M.; Kayastha, V.; Wang, J. S.; Yap, Y. K. Patterned Growth of Boron Nitride Nanotubes by Catalytic Chemical Vapor Deposition. *Chem. Mater.* **2010**, *22*, 1782–1787.
101. Lee, C. H.; Wang, J. H.; Kayashta, V. K.; Huang, J. Y.; Yap, Y. K. Effective Growth of Boron Nitride Nanotubes by Thermal Chemical Vapor Deposition. *Nanotechnology* **2008**, *19*, 455605.
102. Lim, S. H.; Luo, J.; Ji, W.; Lin, J. Synthesis of Boron Nitride Nanotubes and Its Hydrogen Uptake. *Catal. Today* **2007**, *120*, 346–350.
103. Corso, M.; Auwarter, W.; Muntwiler, M.; Tamai, A.; Greber, T.; Osterwalder, J. Boron Nitride Nanomesh. *Science* **2004**, *303*, 217–220.
104. Ng, M. L.; Preobrajenski, A. B.; Vinogradov, A. S.; Martensson, N. Formation and Temperature Evolution of Au Nanoparticles Supported on the h-BN Nanomesh. *Surf. Sci.* **2008**, *602*, 1250–1255.
105. Tang, C. C.; Bando, Y.; Huang, Y.; Yue, S.; Gu, C.; Golberg, D. Fluoridation and Electrical Conductivity of BN Nanotubes. *J. Am. Chem. Soc.* **2005**, *127*, 6552–6553.
106. Wang, W.; Bando, Y.; Zhi, C. Y.; Fu, W.; Wang, E. G.; Golberg, D. Aqueous Noncovalent Functionalization and Controlled Near-Surface Carbon Doping of Multiwallled Boron Nitride Nanotubes. *J. Am. Chem. Soc.* **2008**, *130*, 8144–8145.
107. Bai, X. D.; Golberg, D.; Bando, Y.; Zhi, C. Y.; Tang, C. C.; Mitome, M.; Kurashima, K. Deformation-Driven Electrical Transport of Individual Boron Nitride Nanotubes. *Nano Lett.* **2007**, *7*, 632–637.
108. Zhi, C. Y.; Bando, Y.; Tang, C. C.; Golberg, D. Engineering of Electronic Structure of Boron Nitride Nanotubes by Covalent Functionalization. *Phys. Rev. B* **2006**, *74*, 153413.
109. Chang, C. W.; Fennimore, A. M.; Afanasiev, A.; Okawa, D.; Ikuno, T.; Garcia, H.; Li, D.; Majumdar, A.; Zettl, A. Isotope Effect on the Thermal Conductivity of Boron Nitride Nanotubes. *Phys. Rev. Lett.* **2006**, *97*, 085901.
110. Chang, C. W.; Okawa, D.; Majumdar, A.; Zettl, A. Solid State Thermal Rectifier. *Science* **2006**, *314*, 1121–1124.
111. Wu, J.; Han, W. Q.; Walukiewicz, W.; Ager, J. W.; Shan, W.; Haller, E. E.; Zettl, A. Raman Spectroscopy and Time-Resolved Photoluminescence of BN and $B_xC_yN_z$ Nanotubes. *Nano Lett.* **2004**, *4*, 647–650.
112. Jaffrennou, P.; Barjon, J.; Schmid, T.; Museur, L.; Kanaev, A.; Lauret, J.-S.; Zhi, C. Y.; Tang, C.; Bando, Y.; Golberg, D.; *et al.* Near Band-Edge Recombinations in Multiwalled Boron Nitride Nanotubes: Cathodoluminescence and Photoluminescence Spectroscopy Measurements. *Phys. Rev. B* **2008**, *77*, 235422.
113. Watanabe, K.; Taniguchi, T.; Kanda, H. Direct-Bandgap Properties and Evidence for Ultraviolet Lasing of Hexagonal Boron Nitride Single Crystal. *Nat. Mater.* **2004**, *3*, 404–409.
114. Zhi, C. Y.; Bando, Y.; Tang, C. C.; Golberg, D.; Xie, R. G.; Sekiguchi, T. Phonon Characteristics and Cathodoluminescence of Boron Nitride Nanotubes. *Appl. Phys. Lett.* **2005**, *86*, 213110.
115. Chopra, N. G.; Zettl, A. Measurement of the Elastic Modulus of a Multi-wall Boron Nitride Nanotube. *Solid State Commun.* **1998**, *105*, 297–300.
116. Nakhmanson, S. M.; Calzolari, A.; Meunier, V.; Bernholc, J.; Nardelli, M. B. Spontaneous Polarization and Piezoelectricity in Boron Nitride Nanotubes. *Phys. Rev. B* **2003**, *67*, 235406.
117. Zhi, C. Y.; Bando, Y.; Tang, C. C.; Golberg, D. Immobilization of Proteins on Boron Nitride Nanotubes. *J. Am. Chem. Soc.* **2005**, *127*, 17144–17145.
118. Li, Y. B.; Dorozhkin, P.; Bando, Y.; Golberg, D. Controllable Modification of SiC Nanowires Encapsulated in BN Nanotubes. *Adv. Mater.* **2005**, *17*, 545–548.
119. Elias, A. L.; Rodrigues-Manzo, J. A.; McCarttney, M. R.; Golberg, D.; Zamudio, A.; Balatazar, S. E.; Lopes-Urias, F.; Munoz-Sandoval, E.; Gu, L.; Tang, C. C.; *et al.* Production and Characterization of Single-Crystal FeCo Nanowires Inside Carbon Nanotubes. *Nano Lett.* **2005**, *5*, 467–472.
120. Lin, J.; Huang, Y.; Bando, Y.; Tang, C. C.; Golberg, D. BN Tubular Layers-Sheathed CaS:Eu Nanowires as Stable Red-Light-Emitting Nanophosphors. *Chem. Commun.* **2009**, *43*, 6631–6633.
121. Zhi, C. Y.; Bando, Y.; Terao, T.; Tang, C. C.; Kuwahara, H.; Golberg, D. Towards Highly Thermo-Conductive Electrically Insulating Polymeric Composites with Boron Nitride Nanotubes as Fillers. *Adv. Funct. Mater.* **2009**, *19*, 1857–1862.
122. Terao, T.; Bando, Y.; Mitome, M.; Zhi, C. Y.; Tang, C. C.; Golberg, D. Thermal Conductivity Improvement of Polymer Films by Catechin-Modified Boron Nitride Nanotubes. *J. Phys. Chem. C* **2009**, *113*, 13605–13609.
123. Terao, T.; Zhi, C. Y.; Bando, Y.; Mitome, M.; Tang, C. C.; Golberg, D. Alignment of Boron Nitride Nanotubes in Polymeric Composite Films for Thermal Conductivity Improvement. *J. Phys. Chem. C* **2010**, *114*, 4340–4344.
124. Huang, Q.; Bando, Y.; Zhao, L. P.; Zhi, C. Y.; Golberg, D. pH Sensor Based on Boron Nitride Nanotube. *Nanotechnology* **2009**, *20*, 415501.
125. Lee, C. H.; Drelich, J.; Yap, Y. K. Superhydrophobicity of Boron Nitride Nanotubes Grown on Silicon Substrates. *Langmuir* **2009**, *25*, 4853–4860.
126. Hilder, T. A.; Gordon, D.; Chung, S. H. Boron Nitride Nanotubes Selectively Permeable to Cations or Anions. *Small* **2009**, *5*, 2870–2875.
127. Hilder, T. A.; Gordon, D.; Chung, S. H. Salt Rejection and Water Transport through Boron Nitride Nanotubes. *Small* **2009**, *5*, 2183–2190.
128. Ciofani, G.; Raffa, V.; Yu, J.; Chen, Y.; Obata, Y.; Takeoka, S.; Menciasssi, A.; Cuschieri, A. Boron Nitride Nanotubes: A Novel Vector for Targeted Magnetic Drug Delivery. *Curr. Nanosci.* **2009**, *5*, 33–38.
129. Huang, Y.; Lin, J.; Bando, Y.; Tang, C. C.; Zhi, C. Y.; Shi, Y. G.; Takayama-Muromachi, E.; Golberg, D. BN Nanotubes Coated with Uniformly-Distributed Fe_3O_4 Nanoparticles: Novel Magneto-Operable Nanocomposites. *J. Mater. Chem.* **2010**, *20*, 1007–1011.
130. Yan, B.; Park, C.; Ihm, J.; Zhou, G.; Duan, W.; Park, N. Electron Emission Originated from Free-Electron-like States of Alkali-Doped Boron Nitride Nanotubes. *J. Am. Chem. Soc.* **2008**, *130*, 17012–17015.
131. Golberg, D.; Dorozhkin, P.; Bando, Y.; Dong, Z. C. Synthesis, Analysis and Electrical Property Measurements of Compound Nanotubes in the Ceramic B−C−N System. *MRS Bull.* **2004**, *29*, 38–42.
132. Belonenko, M. B.; Lebedev, N. G. Two-Qubit Cells Made of Boron Nitride Nanotubes for a Quantum Computer. *Tech. Phys.* **2009**, *54*, 338–342.
133. Zhi, C. Y.; Bando, Y.; Tang, C. C.; Golberg, D. SnO_2 Nanoparticle Functionalized BN Nanotubes. *J. Phys. Chem. B* **2006**, *110*, 8548–8550.
134. Chen, X.; Wu, P.; Rousseas, M.; Okawa, D.; Gartner, Z.; Zettl, A.; Bertozzi, C. R. Boron Nitride Nanotubes Are Noncytoxic and Can Be Functionalized for Interaction with Proteins and Cells. *J. Am. Chem. Soc.* **2009**, *131*, 890–891.

135. Ciofani, C.; Raffa, V.; Menciassi, A.; Cuschieri, A. Boron Nitride Nanotubes: An Innovative Tool for Nanomedicine. *Nano Today* **2009**, *4*, 8–10.
136. Yu, J.; Zhang, Q.; Ahn, J.; Yoon, S. F.; Gan, B.; Chew, K.; Tan, K. H.; Bai, X. D.; Wang, E. G. Growth and Structure of Aligned B−C−N Nanotubes. *J. Vac. Sci. Technol., B* **2001**, *19*, 671–674.
137. Terrones, M.; Grobert, N.; Terrones, H. Synthetic Routes to Nanoscale $B_xC_yN_z$ Architectures. *Carbon* **2002**, *40*, 1665–1684.
138. Tanaka, T.; Itoh, A.; Yamashita, K.; Rokuta, E.; Oshima, C. Heteroepitaxial System of h-BN/Monolayere Graphene on Ni(111). *Surf. Rev. Lett.* **2003**, *10*, 697–703.
139. Blase, X.; Charlier, J. C; Vita, A.; De; Car, R. Theory of Composite $B_xC_yN_z$ Nanotube Heterojunctions. *Appl. Phys. Lett.* **1997**, *70*, 197–199.
140. Yu, J.; Ahn, J.; Yoon, S. F.; Zhang, Q; Rusli; Gan, B.; Chew, K; Yu, M. B.; Bai, X. D.; Wang, E. G. Semiconducting Boron Carbonitride Nanostructures: Nanotubes and Nanofibers. *Appl. Phys. Lett.* **2000**, *77*, 1949–1951.
141. Bai, X. D.; Guo, J. D.; Yu, J.; Wang, E. G.; Yuan, J.; Zhou, W. Z. Synthesis and Field-Emission Behavior of Highly Oriented Boron Carbonitride Nanofibers. *Appl. Phys. Lett.* **2000**, *76*, 2624–2626.
142. Choi, J.; Kim, Y. H.; Chang, K. J.; Tomanek, D. Itinerant Ferromagnetism in Heterostructured C/BN Nanotubes. *Phys. Rev. B* **2003**, *67*, 125421.
143. Yaziev, O. V.; Pasquarello, A. Magnetoresistive Junctions Based on Epitaxial Graphene and Hexagonal Boron Nitride. *Phys. Rev. B* **2009**, *80*, 035408.
144. Xu, Z.; Golberg, D.; Bando, Y. *In-Situ* TEM-STM Recorded Kinetics of Boron Nitride Nanotube Failure under Current Flow. *Nano Lett.* **2009**, *9*, 2251–2254.
145. Xu, Z.; Golberg, D.; Bando, Y. Electrical Field-Assisted Thermal Decomposition of Boron Nitride Nanotube: Experiments and First Principle Calculations. *Chem. Phys. Lett.* **2009**, *480*, 110–112.
146. Krivanek, O. L.; Chisholm, M. F.; Nicolosi, V.; Pennycook, T. J.; Corbin, G. J.; Dellby, N.; Murfitt, M. F.; Own, C. S.; Szilagyi, Z. S.; Oxley, M. P.; *et al.* Atom-by-Atom Structural and Chemical Analysis by Annular Dark-Field Electron Microscopy. *Nature* **2010**, *464*, 571–574.